

Sequential Subspace Search for Functional Bayesian Optimization Incorporating Experimenter Intuition

Alistair Shilton, Sunil Gupta, Santu Rana, Svetha Venkatesh

Applied Artificial Intelligence Institute (A2I2)
Deakin University, Geelong, Australia
alistair.shilton@deakin.edu.au

Abstract

We propose an algorithm for Bayesian functional optimisation - that is, finding the function to optimise a process - guided by experimenter beliefs and intuitions regarding the expected characteristics (length-scale, smoothness, cyclicity etc.) of the optimal solution encoded into the covariance function of a Gaussian Process. Our algorithm generates a sequence of finite-dimensional random subspaces of functional space spanned by a set of draws from the experimenter’s Gaussian Process. Standard Bayesian optimisation is applied on each subspace, and the best solution found used as a starting point (origin) for the next subspace. Using the concept of effective dimensionality, we analyse the convergence of our algorithm and provide a regret bound to show that our algorithm converges in sub-linear time provided a finite effective dimension exists. We test our algorithm in simulated and real-world experiments, namely blind function matching, finding the optimal precipitation-strengthening function for an aluminium alloy, and learning rate schedule optimisation for deep networks.

1 Introduction

Functional optimisation arises in circumstances where we seek to optimise continuously varying phenomena. For example we may wish to optimise the curve of an aeroplane’s wing to minimise drag and maximise lift, define the optimal tempering profile (temperature as a function of time) to maximise the strength of an alloy, or find the activation function that works best in a neural network. A common characteristics in these examples is that evaluating the performance of a particular function is (a) expensive (for example fabricating a wing or training and evaluating a deep network) and (b) results in a noisy measurement. Furthermore we often have a beliefs regarding the characteristics that will perform best in a given circumstance. For example physical intuition may tell us that a plane’s wing should vary on a length-scale of meters, and that sharp points are likely to degrade performance.

Two related works in the area of functional Bayesian optimisation are [Vien et al. 2018] and control function optimisation [Vellanki et al. 2019]. In [Vien et al. 2018] functions are represented as elements in a reproducing kernel Hilbert space (RKHS). At each iteration an acquisition functional is optimised using (Frechet) gradient descent (with multi-start at a random initial point to avoid local minima), the objective evaluated, models updated and the process repeated. However, experimenter beliefs about the solution only guide the

optimisation procedure indirectly. Alternatively, [Vellanki et al. 2019] searches the space of Bernstein polynomials of (at most) a particular degree, where strong *shape function* constraints can be enforced. Shape priors include priors on monotonicity, unimodality, and other properties that may be expressed as constraints on the Bernstein basis of the solution, but not the looser beliefs that we are concerned with here (e.g. the expected length-scale of variation of a plane’s wing, the smoothness of our solution (lack of sharp edges, or otherwise), stationarity of form etc).

In this paper we propose an algorithm to solve expensive functional optimisation problems with beliefs on the solution expressed as a Gaussian Process covariance function, allowing us to encode “loose” beliefs and intuitions regarding for example length-scales, smoothness, and cyclicity of the optimal solution. We note in passing that, while our primary focus is on the encoding of beliefs/intuitions of this form, in principle it is possible to encode harder “shape priors” using our approach. For example monotonicity may be enforced in the Gaussian Process [Riihimäki and Vehtari 2010], and some relevant physical constraints may be directly built into covariance functions [Jidling et al. 2017]. We also provide a sub-linear regret bound to assure the performance of our algorithm through the concept of equivalent dimension.

The approach we take is to construct a sequence of low-dimensional search spaces by sampling the Gaussian process encoding our beliefs regarding the optimal solution to define a function basis (REMBO style [Wang et al. 2013]), and then use Bayesian optimisation to find the best solution (function) in this subspace. This solution (function) then becomes the origin in our next (random) subspace (similar to LineBO [Kirschner et al. 2019]), and the process repeats until the experimental budget is exhausted. By defining our search spaces using samples from a GP encoding our beliefs regarding the solution we give preference to subspaces that satisfy our expectations of the solution - for example if choose a GP with a long lengthscale SE covariance then our search subspaces will tend (on average) to span slowly varying, smooth functions, accelerating optimisation.

In our experiments, we begin by testing our algorithm on blind function matching. This allows us to explore the performance of our algorithm under idealised conditions. We then test of these results carry over into real-world conditions by considering two real-world problems, namely find-

ing the optimal heat-treatment function for Al-Sc (aluminium-scandium) alloy to maximise its strength, and obtaining the optimal learning-rate schedule for training a deep network.

1.1 Notation

We use $\mathbb{N} = \{0, 1, \dots\}$, $\mathbb{N}_i = \{0, 1, \dots, i - 1\}$ and $\text{span}(x_0, x_1, \dots) = \{\sum_i \alpha_i x_i \mid \alpha_i \in \mathbb{R}\}$. $|\mathbb{D}|$ is the number of elements in a finite set \mathbb{D} . $L_2(\mathbb{B})$ is the set of L_2 -integrable functions $f : \mathbb{B} \rightarrow \mathbb{R}$, and $\mathcal{H}_K(\mathbb{B})$ the Reproducing-Kernel Hilbert Space [Aronszajn 1950] with reproducing kernel $K : \mathbb{B} \times \mathbb{B} \rightarrow \mathbb{R}$. Column vectors are $\mathbf{a}, \mathbf{b}, \dots$ and matrices $\mathbf{V}, \mathbf{W}, \dots$, with elements $a_i, \dots, W_{i,j}, \dots$. $\mathbf{a} \odot \mathbf{b}$ is the element-wise product. $\llbracket \cdot \rrbracket$ is the Iverson bracket [Iverson 1962] (for bool q , $\llbracket q \rrbracket = 1$ if q true, 0 otherwise).

2 Problem Statement

This paper is concerned with solving the problem:

$$\mathbf{g}^* = \underset{\mathbf{g} \sim \mathcal{GP}(0, \kappa) : \|\mathbf{g}\|_{L_2(\mathbb{A})} \leq L_{\max}}{\text{argmax}} f(\mathbf{g}) \quad (1)$$

where $f : L_2(\mathbb{A}) \rightarrow \mathbb{R}$ is an expensive (to evaluate) and noisy functional. That is, we want to find the *function* $\mathbf{g} : \mathbb{A} \rightarrow \mathbb{R}$ that produces the best results when applied in some process f - e.g. we may wish to find the best activation function for a neural network or the best temperature profile to optimise the properties of an alloy.

By assuming $\mathbf{g}^* \sim \mathcal{GP}(0, \kappa)$ is a draw from a zero-mean Gaussian Process characterised by the covariance function $\kappa : \mathbb{A} \times \mathbb{A} \rightarrow \mathbb{R}$, the experimenter may assert beliefs and intuitions regarding the properties of \mathbf{g} through the selection of the covariance κ . For example, the length-scale, smoothness and periodicity characteristics of κ control the length-scale, smoothness and periodicity characteristics of \mathbf{g}^* , allowing the experimenter to specify how quickly the temperature may change in an annealing process, or how smooth the surface of a wing is. This is in contrast to the strong ‘‘shape priors’’ of [Vellanki et al. 2019], which allows strong constraints on \mathbf{g} such as monotonicity and unimodality to be enforced, but not looser beliefs on e.g. length-scale and periodicity.

3 Background

3.1 Gaussian Processes

A Gaussian process $\mathcal{GP}(\mu, K)$ is a distribution on a space of functions $f : \mathbb{X} \rightarrow \mathbb{R}$ with mean $\mu : \mathbb{X} \rightarrow \mathbb{R}$ and covariance $K : \mathbb{X} \times \mathbb{X} \rightarrow \mathbb{R}$ [MacKay 1998, Rasmussen and Williams 2006]. Let $f \sim \mathcal{GP}(\mu, K)$ be a draw from a Gaussian process. Then the posterior of f given noisy observations $\mathbb{D} = \{(x_i, y_i) \mid y_i = f(x_i) + \epsilon_i, \epsilon_i \sim \mathcal{N}(0, \sigma^2)\}$ is $f(x) \mid \mathbb{D} \sim \mathcal{N}(\mu_{\mathbb{D}}(x), \sigma_{\mathbb{D}}^2(x))$, where $\sigma_{\mathbb{D}}^2(x) = K_{\mathbb{D}}(x, x)$, $K_{\mathbb{D}}(x, x')$ is the posterior covariance:

$$\begin{aligned} \mu_{\mathbb{D}}(x) &= \mu(x) + K(x, \mathbb{D}) (K(\mathbb{D}, \mathbb{D}) + \sigma^2 \mathbf{I})^{-1} (\mathbf{y} - \mu(\mathbb{D})) \\ K_{\mathbb{D}}(x, x') &= K(x, x') - K(x, \mathbb{D}) (K(\mathbb{D}, \mathbb{D}) + \sigma^2 \mathbf{I})^{-1} K(\mathbb{D}, x') \end{aligned} \quad (2)$$

and we use the shorthand notations:

$$\begin{aligned} \mu(\mathbb{D}) &= [\mu(x_i)]_{i \in \mathbb{N}_{|\mathbb{D}|}}^T, \quad K(\mathbb{D}, \mathbb{D}) = [K(x_i, x_j)]_{i, j \in \mathbb{N}_{|\mathbb{D}|}} \\ K(x, \mathbb{D}) &= K(\mathbb{D}, x)^T = [K(x, x_i)] \end{aligned}$$

Note that this applies to functions $f : \mathbb{X} \rightarrow \mathbb{R}$ for any \mathbb{X} on which a covariance $K : \mathbb{X} \times \mathbb{X} \rightarrow \mathbb{R}$ can be defined.

Algorithm 1 Standard Bayesian Optimisation.

input Prior $K : \mathbb{X} \times \mathbb{X} \rightarrow \mathbb{R}$ on $f \sim \mathcal{GP}(0, K)$.
Initial observations $\mathbb{D} = \{(\mathbf{x}, y = f(\mathbf{x}) + \epsilon) \mid \mathbf{x} \sim \mathcal{D}_{\mathbb{A}}, \epsilon \sim \mathcal{N}(0, \sigma^2)\}$ (for distribution $\mathcal{D}_{\mathbb{A}}$).
Modelling $f \sim \mathcal{GP}(0, K)$, proceed:
for $t = 0, 1, \dots$ until converged on \mathbb{X} **do**
 Solve $\mathbf{x} \leftarrow \text{argmax}_{\mathbf{x} \in \mathbb{X}} a_t(\mathbf{x} \mid \mathbb{D})$.
 Observe $y \leftarrow f(\mathbf{x}) + \epsilon, \epsilon \sim \mathcal{N}(0, \sigma^2)$.
 Update $\mathbb{D} \leftarrow \mathbb{D} \cup \{(\mathbf{x}, y)\}$.
end for
Return $(\mathbf{x}^*, y^*) = \text{argmax}_{(\mathbf{x}, y) \in \mathbb{D}} y$.

3.2 Standard Bayesian Optimisation

Typically Bayesian optimisation is concerned with solving:

$$\mathbf{x}^* = \underset{\mathbf{x} \in \mathbb{X} \subseteq \mathbb{R}^n}{\text{argmax}} f(\mathbf{x}) \quad (3)$$

where f is expensive to evaluate and observations are noisy. The aim is to solve (3) using the minimum evaluations of f . Modelling $f \sim \mathcal{GP}(0, K)$ as a draw from a Gaussian process, Bayesian optimisation [Jones et al. 1998] is an iterative algorithm (algorithm 1) for solving (3). At each iteration a (computationally cheap) surrogate acquisition function based on the GP model is optimised to select the next sample point, an observation is made at that point, and the GP model updated. The algorithm terminates either when some termination condition is satisfied or the budget (number of times f may be evaluated) is reached. Popular acquisition functions include probability of improvement [Kushner 1964], expected improvement [Mockus 2002] and Gaussian process upper confidence bound (GP-UCB) [Srinivas et al. 2012]. In this paper we use the GP-UCB acquisition function (of course others could be substituted):

$$a_t(\mathbf{x} \mid \mathbb{D}) = \mu_{\mathbb{D}}(\mathbf{x}) + \sqrt{\beta_t} \sigma_{\mathbb{D}}(\mathbf{x})$$

where β_t are a sequence of constants (see [Srinivas et al. 2012, Brochu et al. 2010] for details). In practice we find that the β_t recommended by [Brochu et al. 2010, page 16] works well in our case without requiring many additional parameters to be selected.

4 Method

Recall that we are concerned with solving (1):

$$\mathbf{g}^* = \underset{\mathbf{g} \sim \mathcal{GP}(0, \kappa) : \|\mathbf{g}\|_{L_2(\mathbb{A})} \leq L_{\max}}{\text{argmax}} f(\mathbf{g})$$

where $f : L_2(\mathbb{A}) \rightarrow \mathbb{R}$ is an expensive (to evaluate) and noisy functional and $\mathbf{g}^* \sim \mathcal{GP}(0, \kappa)$, where κ characterises our expectations on the solution \mathbf{g}^* (e.g. the time-scale at which the temperature profile of the heat-treatment process varies, the smoothness of the plane’s wing). We model $f \sim \mathcal{GP}(0, K)$, and K is our prior over the objective function f .

In standard Bayesian optimisation the search space is most often a finite-dimensional vector space \mathbb{R}^d . For practical reasons (e.g. computational complexity of global optimisation of the acquisition function) early work concentrated on the low-dimensional case, roughly $d \lesssim 10$. Recently progress has

been made in the high dimensional case, typically by the construction of either a single low-dimensional embedded subspace of the search space or a sequence of low-dimensional embedded subspaces on which standard (low-dimensional) optimisation may proceed. For example, REMBO [Wang et al. 2013] constructs a single subspace by random embedding and applies Bayesian Optimisation to this subspace, while LineBO [Kirschner et al. 2019] constructs a sequence of 1-dimensional subspaces (lines), optimising on each before proceeding to the next in a principled manner.

Functional Bayesian Optimisation represents the logical extension of high-dimensional Bayesian optimisation to the infinite dimensional case, where the discrete index $i \in \mathbb{N}_n$ identifying element x_i of vector $\mathbf{x} \in \mathbb{R}^n$ is supplanted by the continuous argument $a \in \mathbb{A}$ in the evaluation $\mathbf{g}(a)$ of function $\mathbf{g} \in L_2(\mathbb{A})$. However one may still apply subspace methods analogous to REMBO and LineBO - for example, as observed in [Vien et al. 2018], random RKHS vectors may be used to define a basis for a subspace $\mathbb{T} \subset L_2(\mathbb{A})$, and optimisation may proceed on \mathbb{T} as it has an (effectively) finite dimension. Alternatively, [Vellanki et al. 2019] uses Bernstein polynomials to span a subspace $\mathbb{U} \subset L_2(\mathbb{A})$, where optimisation may proceed as \mathbb{U} has an (effectively) finite dimension. However neither of these approaches provide a clear means of using our loose priors (as opposed to “hard” shape priors [Vellanki et al. 2019]) on \mathbf{g}^* to accelerate the optimisation procedure.

Motivated by this, our algorithm (section 4.2) is a hybrid extension of REMBO and LineBO. The *outer loop* selects a sequence of S (S is the outer-loop budget) d -dimensional subspaces (as in LineBO, but multi-dimensional) by sampling from $\mathcal{GP}(0, \kappa)$ to generate a finite basis for $\mathbb{U}_s = \mathbf{b}_s + \text{span}(\mathbf{h}_s^0, \mathbf{h}_s^1, \dots, \mathbf{h}_s^{d-1}) \subset L_2(\mathbb{A})$, where $s \in \mathbb{N}_S$ is an iteration count, \mathbf{b}_s is the best solution found up to iteration s , and $\mathbf{h}_s^0, \mathbf{h}_s^1, \dots, \mathbf{h}_s^{d-1} \sim \mathcal{GP}(0, \kappa)$ that favours functions with the characteristics we expect in \mathbf{g}^* , while the *inner loop* searches \mathbb{U}_s using standard Bayesian Optimisation. Note that:

1. The algorithm uses two distinct covariance functions:
 - (a) Covariance κ guides subspace selection for each outer loop iteration s , guiding the algorithm to explore subspaces of functions with characteristics we expect of \mathbf{g}^* .
 - (b) Covariance K characterises the functional space, which we discuss in detail in section 4.1.
2. Each function \mathbf{g} evaluated in the inner loop is a weighted sum of the basis functions $\mathbf{h}_s^0, \mathbf{h}_s^1, \dots, \mathbf{h}_s^{d-1}$, and, recursively through the bias \mathbf{b}_s , all previous such bases. This sum contains at most dS terms. In our implementation we use pre-sampling and caching to avoid computational issues arising from this as described in the supplementary.
3. Convergence of the inner loop can be assessed using either a simple budget of T evaluations (resulting in ST evaluations overall over S outer loop iterations) or a simple regret test as per LineBO [Kirschner et al. 2019] to terminate the inner loop if $\text{err}(\mathbf{g}_s^*) < \epsilon$, where:

$$\text{err}(\mathbf{g}) = \mu_{\mathbb{D}}(\mathbf{g}) + \sigma_{\mathbb{D}}(\mathbf{g}) - \min_{\mathbf{g}' \in \mathbb{U}_s} (\mu_{\mathbb{D}}(\mathbf{g}') - \sigma_{\mathbb{D}}(\mathbf{g}'))$$

4.1 Modelling the Objective

In our algorithm we model f as a draw from a zero-mean Gaussian Process $f \sim \mathcal{GP}(0, K)$, where $K : L_2(\mathbb{A}) \times L_2(\mathbb{A}) \rightarrow \mathbb{R}$. This necessitates the construction of an appropriate covariance K . Two potential approaches to constructing this covariance are:

1. As per [Vien et al. 2018], build $K : \mathcal{H}_{\kappa}(\mathbb{A}) \times \mathcal{H}_{\kappa}(\mathbb{A}) \rightarrow \mathbb{R}$ on the RKHS $\mathcal{H}_{\kappa}(\mathbb{A})$ by taking a stationary covariance on \mathbb{R}^d and replacing $\|\mathbf{x} - \mathbf{x}'\|_2^2$ with $\|\mathbf{g} - \mathbf{g}'\|_{\mathcal{H}_{\kappa}(\mathbb{A})}^2$. For example:

$$K(\mathbf{g}, \mathbf{g}') = \exp\left(-\frac{1}{2\gamma^2} \|\mathbf{g} - \mathbf{g}'\|_{\mathcal{H}_{\kappa}(\mathbb{A})}^2\right) \quad (4)$$

2. Noting that $L_2(\mathbb{A})$ is a Hilbert space, build $K : L_2(\mathbb{A}) \times L_2(\mathbb{A}) \rightarrow \mathbb{R}$ by taking a stationary covariance on \mathbb{R}^d and replacing $\|\mathbf{x} - \mathbf{x}'\|_2^2$ with $\|\mathbf{g} - \mathbf{g}'\|_{L_2(\mathbb{A})}^2$. For example:

$$K(\mathbf{g}, \mathbf{g}') = \exp\left(-\frac{1}{2\gamma^2} \|\mathbf{g} - \mathbf{g}'\|_{L_2(\mathbb{A})}^2\right) \quad (5)$$

Both approaches require numerical approximation. In the first approach, functions $\mathbf{g}, \mathbf{g}' \in L_2(\mathbb{A})$ must be approximated as $\mathbf{g} \approx \sum_i \alpha_i \kappa(\cdot, \mathbf{c}^i)$, $\mathbf{g}' \approx \sum_i \alpha'_i \kappa(\cdot, \mathbf{c}^i)$ for a suitable grid of points $\mathbf{c}^i \in \mathbb{A}$ (e.g. an even grid of $N^{1/m}$ points per axis in $\mathbb{A} \subset \mathbb{R}^m$ with spacing τ), so:

$$\|\mathbf{g} - \mathbf{g}'\|_{\mathcal{H}_{\kappa}(\mathbb{A})}^2 \approx \sum_{i,j} (\alpha_i - \alpha'_i)(\alpha_j - \alpha'_j) \kappa(\mathbf{c}^i, \mathbf{c}^j) \quad (6)$$

Likewise in approach 2, using the same grid, we may use a histogram approximation:

$$\|\mathbf{g} - \mathbf{g}'\|_{L_2(\mathbb{A})}^2 \approx \sum_i (\mathbf{g}(\mathbf{c}^i) - \mathbf{g}'(\mathbf{c}^i))^2 \tau^m \quad (7)$$

The computational cost of the first approach scales quadratically with the size N of the grid, whereas approach 2 scales linearly. Furthermore approach 1 conflates two distinct beliefs, namely (a) our beliefs regarding the expected properties of the $\mathbf{g}^* \sim \mathcal{GP}(0, \kappa)$ (smoothness, length-scale etc), and (b) our prior regarding the characteristics of the objective $f \sim \mathcal{GP}(0, K)$, as the recipe for approach 1 embeds the former into the latter via (6) in the construction of K . However there is no a-priori reason to link these concepts, or presume that such linking will improve convergence.

By contrast the approach we have selected (approach 2) builds K from the (solution, or κ -) belief agnostic function-difference measure $\|\mathbf{g} - \mathbf{g}'\|_{L_2(\mathbb{A})}$, so κ and K serve two distinct purposes: κ guides our choice of search sub-space, giving preference to subspaces containing mostly functions that we expect to be similar to the optimal solution \mathbf{g}^* ; and K is used to model our objective function f .

We discuss how (7) may be efficiently computed using a grid approximation in the supplementary material. For practical purposes, we note that the computational cost of this approximation on our algorithm scales linearly with the grid-size N , so the penalty for “overdoing it” to ensure an accurate approximation is relatively small (for example in our experiments we use $N = 100$ without difficulty), so we recommend being generous in this respect. If the grid is too small then the effect will be similar to choosing a length-scale on K that is too large, as an overly coarse grid will be unable to capture fine (sharp) features in \mathbf{g} (effectively calculating

Algorithm 2 Sequential-Subspace-Search Bayesian Functional Optimisation (S^3 -BFO) Algorithm.¹

input Prior $K : L_2(\mathbb{A}) \times L_2(\mathbb{A}) \rightarrow \mathbb{R}$ on $f \sim \mathcal{GP}(0, K)$.

input Prior $\kappa : \mathbb{A} \times \mathbb{A} \rightarrow \mathbb{R}$ on $\mathbf{g}^* \sim \mathcal{GP}(0, \kappa)$.

Let $(\mathbf{g}_{[0]}^*, y_{[0]}^*) = (0, 0)$.

Modelling $f \sim \mathcal{GP}(0, K)$, proceed:

for $s = 0, 1, \dots, S - 1$ **do** (outer loop)

Assign $\mathbf{b}_s \leftarrow \mathbf{g}_{[s]}^*$.

Sample $\mathbf{h}_s^0, \mathbf{h}_s^1, \dots, \mathbf{h}_s^{d-1} \sim \mathcal{GP}(0, \kappa)$.

Initial observations $\mathbf{D}_s = \{(\mathbf{g} = \mathbf{b}_s + \sum_j \lambda_j \mathbf{h}_s^j, y = f(\mathbf{g}) + \epsilon) \mid \lambda \sim \mathcal{D}_{\mathbb{R}^d}, \epsilon \sim \mathcal{N}(0, \sigma^2)\}$.

for $t = 0, 1, \dots$ until converged on \mathbb{U}_s **do** (inner loop)

Solve $\lambda \leftarrow \operatorname{argmax}_{\lambda \in \mathbb{R}^d} a_t(\mathbf{b}_s + \sum_j \lambda_j \mathbf{h}_s^j \mid \mathbf{D}_{[s]} \cup \mathbf{D}_s)$.

Project $\mathbf{g} \leftarrow \mathbf{b}_s + \sum_j \lambda_j \mathbf{h}_s^j$.

Observe $y \leftarrow f(\mathbf{g}) + \epsilon, \epsilon \sim \mathcal{N}(0, \sigma^2)$.

Update $\mathbf{D}_s \leftarrow \mathbf{D}_s \cup \{(\mathbf{g}, y)\}$.

end for

Let $\mathbf{D}_{[s+1]} = \mathbf{D}_{[s]} \cup \mathbf{D}_s$.

Let $(\mathbf{g}_{[s+1]}^*, y_{[s+1]}^*) = \operatorname{argmax}_{(\mathbf{g}, y) \in \mathbf{D}_{[s+1]}} y$.

end for

Return $(\mathbf{g}_{[S]}^*, y_{[S]}^*)$.

the difference smoothed approximations). Finally, we implicitly assume a low-dimensional domain $\mathbb{A} = \mathbb{R}^\nu$ for \mathbf{g} (practically $\nu \leq 3$). This captures many physical cases of interest like scheduling ($\nu = 1$) or wing design ($\nu = 2$) while still retaining a practical grid size $N = \rho^\nu$. The extension to higher dimensions will require some additional approximation of \mathbf{g} to keep the computational cost within sensible bounds, but this is beyond the scope of the present paper.

4.2 The Algorithm

Our proposed algorithm is shown in algorithm 2. As noted previously, the *outer loop* selects a sequence of subspaces by drawing a basis $\mathbf{h}_s^0, \mathbf{h}_s^1, \dots, \mathbf{h}_s^{d-1} \sim \mathcal{GP}(0, \kappa)$ to define a subspace $\mathbb{U}_s = \mathbf{b}_s + \operatorname{span}(\mathbf{h}_s^0, \mathbf{h}_s^1, \dots, \mathbf{h}_s^{d-1})$ that is biased to favour functions with the characteristics we expect of the optima $\mathbf{g}^* \sim \mathcal{GP}(0, \kappa)$. The *inner loop* uses standard Bayesian Optimisation with a GP-UCB acquisition function to find the best solution on this subspace, which then becomes the bias \mathbf{b}_{s+1} for the next outer-loop iteration, and so on. The selection of the subspace dimension d is discussed in section 5.2, but loosely speaking $1 \leq d \leq \max(10, d_e)$, where $d = 1$ makes the algorithm behave like LineBO, $d = d_e$ makes it behave like REMBO, d_e is the effective dimension of the objective f (definition 1, though this is rarely known), and 10 is the practical upper-bound for computational reasons. The hyperparameters for covariance K are tuned for max-log-likelihood in the usual manner.

¹For clarity, when reading this algorithm, note that the super/subscript s implies “for iteration s ”, whereas the super/subscript $[s]$ implies “up to but not including iteration s ”, so for example \mathbf{D}_s is the set of observations made during iteration s , whereas $\mathbf{D}_{[s]}$ is the set of all observations made prior to iteration s .

5 Convergence Analysis

As in the analysis of REMBO and LineBO, our convergence analysis is based around the concept of *effective dimensionality*. For the functional case we define this as follows:

Definition 1 Let $f : L_2(\mathbb{A}) \rightarrow \mathbb{R}$. The *effective dimension* of f is the lowest $d_e \in \mathbb{N}$ such that there exists $\bar{\mathbf{h}}^0, \bar{\mathbf{h}}^1, \dots, \bar{\mathbf{h}}^{d_e-1} \in L_2(\mathbb{A})$ such that $\|f(\mathbf{g} + \mathbf{g}_\perp) - f(\mathbf{g})\|_{L_2(\mathbb{A})} = 0 \forall \mathbf{g} \in \mathbb{T}, \forall \mathbf{g}_\perp \in \mathbb{T}^\perp$, where $\mathbb{T} = \operatorname{span}(\bar{\mathbf{h}}^0, \bar{\mathbf{h}}^1, \dots, \bar{\mathbf{h}}^{d_e-1})$.

In our analysis of algorithm 2 we first consider the inner and outer loops separately. The inner-loop may be analysed in terms of the standard BO optimisation using GP-UCB acquisition function [Srinivas et al. 2012]; whereas the outer loop analysis more closely models the analysis of LineBO in [Kirschner et al. 2019].

5.1 Inner-Loop Convergence

Our aim here is to bound cumulative regret bound $R_t = \sum_{t'} (f(\mathbf{g}^*) - f(\mathbf{g}^{t'}))$ on the inner loop of algorithm 2 in terms of the inner-loop iteration counter t . The complicating factors are:

1. The model is not built on the variables optimised by the inner loop (the λ 's) but rather the projection of these objects into function space (the \mathbf{g} 's).
2. The model used for f is built from not just the current instance of the inner loop but all previous instances.

With regard to point 1, note that, in terms of our basis \mathbb{U}_s , we can rewrite $\|\mathbf{g} - \mathbf{g}'\|_2^2$ as:

$$\begin{aligned} \|\mathbf{g} - \mathbf{g}'\|_{L_2(\mathbb{A})}^2 &= \|\sum_i (\lambda_i - \lambda'_i) \mathbf{h}_s^i\|_{L_2(\mathbb{A})}^2 \\ &= (\boldsymbol{\lambda} - \boldsymbol{\lambda}')^T \mathbf{H}^s (\boldsymbol{\lambda} - \boldsymbol{\lambda}') \end{aligned}$$

where $\mathbf{H}^s \succeq \mathbf{0}$, $H_{ij}^s = \langle \mathbf{h}_s^i, \mathbf{h}_s^j \rangle_{L_2(\mathbb{A})}$, which has the form of a Mahalanobis distance. But this is equivalent to a standard Euclidean distance operating on data that has been appropriately scaled and rotated. In particular, the maximum information gain [Cover and Thomas 1991] γ_t of a covariance function depends only on the number of observations and not how they have been rotated and/or scaled. Thus if we construct our covariance function K by taking a translation-invariant covariance on \mathbb{R}^d with now maximum information gain and then translating it to a covariance on $L_2(\mathbb{A})$ then the maximum information gain of the resulting covariance will be the same as for the original.

With regard to point 2, recall that the posterior of $f \sim \mathcal{GP}(0, K)$ at outer iteration s prior to entering the inner loop is $f(\mathbf{g}) \mid \mathbf{D}_{[s]} \sim \mathcal{N}(\mu_{\mathbf{D}_{[s]}}(\mathbf{g}), \sigma_{\mathbf{D}_{[s]}}^2(\mathbf{g}))$ as per (2). Similarly, at iteration t in the inner loop the posterior of $f \sim \mathcal{GP}(0, K)$ is $f(\mathbf{g}) \mid \mathbf{D}_{[s]} \cup \mathbf{D}_s \sim \mathcal{N}(\mu_{\mathbf{D}_{[s]} \cup \mathbf{D}_s}(\mathbf{g}), \sigma_{\mathbf{D}_{[s]} \cup \mathbf{D}_s}^2(\mathbf{g}))$ as per (2). See figure 1, it is not difficult to show that this posterior is equivalent to the posterior of $f \sim \mathcal{GP}(\mu_{\mathbf{D}_{[s]}}, K_{\mathbf{D}_{[s]}})$ given \mathbf{D}_s - the posterior of the biased GP whose prior covariance is $K_{\mathbf{D}_{[s]}}$.

Hence, for outer-loop iteration s , the inner loop is essentially standard GP-UCB BO, [Srinivas et al. 2012], but with covariance prior $K_{\mathbf{D}_{[s]}}$. Denoting by $\gamma_{\mathbf{D}_{[s]}, t}$ the maximum information gain for this covariance function, we have from

By definition, the posterior mean and variance of $f \sim \mathcal{GP}(0, K)$ given $\mathcal{D}_{[s]} \cup \mathcal{D}_s$ are:

$$\begin{aligned}\mu_{\mathcal{D}_{[s]} \cup \mathcal{D}_s}(\mathbf{g}) &= \begin{bmatrix} K(\mathcal{D}_{[s]}, \mathbf{g}) \\ K(\mathcal{D}_s, \mathbf{g}) \end{bmatrix}^T \begin{bmatrix} K(\mathcal{D}_{[s]}, \mathcal{D}_{[s]}) + \sigma^2 \mathbf{I} & K(\mathcal{D}_{[s]}, \mathcal{D}_s) \\ K(\mathcal{D}_s, \mathcal{D}_{[s]}) & K(\mathcal{D}_s, \mathcal{D}_s) + \sigma^2 \mathbf{I} \end{bmatrix}^{-1} \begin{bmatrix} \mathbf{y}_{\mathcal{D}_{[s]}} \\ \mathbf{y}_{\mathcal{D}_s} \end{bmatrix} \\ \sigma_{\mathcal{D}_{[s]} \cup \mathcal{D}_s}^2(\mathbf{g}) &= K(\mathbf{g}, \mathbf{g}) - \begin{bmatrix} K(\mathcal{D}_{[s]}, \mathbf{g}) \\ K(\mathcal{D}_s, \mathbf{g}) \end{bmatrix}^T \begin{bmatrix} K(\mathcal{D}_{[s]}, \mathcal{D}_{[s]}) + \sigma^2 \mathbf{I} & K(\mathcal{D}_{[s]}, \mathcal{D}_s) \\ K(\mathcal{D}_s, \mathcal{D}_{[s]}) & K(\mathcal{D}_s, \mathcal{D}_s) + \sigma^2 \mathbf{I} \end{bmatrix}^{-1} \begin{bmatrix} K(\mathcal{D}_{[s]}, \mathbf{g}) \\ K(\mathcal{D}_s, \mathbf{g}) \end{bmatrix}\end{aligned}$$

Likewise, the posterior mean and covariance of $f \sim \mathcal{GP}(0, K)$ given only $\mathcal{D}_{[s]}$ are:

$$\begin{aligned}\mu_{\mathcal{D}_{[s]}}(\mathbf{g}) &= K(\mathbf{g}, \mathcal{D}_{[s]}) (K(\mathcal{D}_{[s]}, \mathcal{D}_{[s]}) + \sigma^2 \mathbf{I})^{-1} \mathbf{y}_{\mathcal{D}_{[s]}} \\ K_{\mathcal{D}_{[s]}}^2(\mathbf{g}, \mathbf{g}') &= K(\mathbf{g}, \mathbf{g}') - K(\mathbf{g}, \mathcal{D}_{[s]}) (K(\mathcal{D}_{[s]}, \mathcal{D}_{[s]}) + \sigma^2 \mathbf{I})^{-1} K(\mathcal{D}_{[s]}, \mathbf{g}')\end{aligned}$$

Using the matrix inversion lemma, it is straightforward to rewrite the former in terms of the latter:

$$\begin{aligned}\mu_{\mathcal{D}_{[s]} \cup \mathcal{D}_s}(\mathbf{g}) &= \mu_{\mathcal{D}_{[s]}}(\mathcal{D}_s) + K_{\mathcal{D}_{[s]}}(\mathbf{g}, \mathcal{D}_s) (K_{\mathcal{D}_{[s]}}(\mathcal{D}_s, \mathcal{D}_s) + \sigma^2 \mathbf{I})^{-1} (\mathbf{y}_{\mathcal{D}_s} - \mu_{\mathcal{D}_{[s]}}(\mathcal{D}_s)) \\ \sigma_{\mathcal{D}_{[s]} \cup \mathcal{D}_s}^2(\mathbf{g}) &= K_{\mathcal{D}_{[s]}}(\mathbf{g}, \mathbf{g}) - K_{\mathcal{D}_{[s]}}(\mathbf{g}, \mathcal{D}_s) (K_{\mathcal{D}_{[s]}}(\mathcal{D}_s, \mathcal{D}_s) + \sigma^2 \mathbf{I})^{-1} K_{\mathcal{D}_{[s]}}(\mathcal{D}_s, \mathbf{g})\end{aligned}$$

Figure 1: Derivation of posterior distribution of f in the inner loop of algorithm 2 in terms of \mathcal{D}_s .

[Srinivas et al. 2012], theorem 2, that the regret for the inner loop of our algorithm goes as:

$$\mathcal{O}^* \left(\sqrt{dt \gamma_{\mathcal{D}_{[s]}, t}} \right)$$

where we follow the notation of [Srinivas et al. 2012] in using \mathcal{O}^* to denote \mathcal{O} with log factors suppressed. Let γ_t be the maximum information gain for covariance K . Clearly $\gamma_{\mathcal{D}_{[s]}, t} = \gamma_{sT+t}$, and moreover we have seen that the maximum information gain of K is precisely the maximum information gain of the non-functional covariance from which it was constructed. Hence for some standard covariance functions we have the bounds [Seeger et al. 2008, Srinivas et al. 2012]:

- Linear: $\gamma_{\mathcal{D}_{[s]}, t} \in \mathcal{O}(d \log t)$.
- Squared exponential: $\gamma_{\mathcal{D}_{[s]}, t} \in \mathcal{O}((\log t)^{d+1})$.
- Matern $\nu > 1$: $\gamma_{\mathcal{D}_{[s]}, t} \in \mathcal{O}(t^{\frac{d(d+1)}{2\nu+d(d+1)}} \log t)$.

where we have used the fact that $\log(sT+t) = \log t + \log(1 + \frac{sT}{t}) \in \mathcal{O}(\log t)$ in this construction (s being fixed for any given instance of the inner loop).

5.2 Outer-Loop and Overall Convergence

With regard to the outer-loop convergence we have the following result, which is analogous to Proposition 1 in [Kirschner et al. 2019] and considers on the number of (outer-loop) iterations the algorithm performs:

Theorem 1 *Let $f \sim \mathcal{GP}(0, K)$ be a draw from a Gaussian Process with twice Frechet-differentiable covariance $K : L_2(\mathbb{A}) \times L_2(\mathbb{A}) \rightarrow \mathbb{R}$ with effective dimension d_e and maxima $\mathbf{g}^* = \arg \max_{\mathbf{g} \in L_2(\mathbb{A})} f(\mathbf{g})$, and let $\delta \in (0, 1)$. Then, using the notation of algorithm 2, after s (outer-loop) iterations of algorithm 2, with probability at least $1 - \delta$:*

$$f(\mathbf{g}^*) - f(\mathbf{g}_{[s]}^*) \in \mathcal{O}(\llbracket d < d_e \rrbracket \left(\frac{1}{s} \log \left(\frac{1}{\delta} \right) \right)^{\frac{2}{d_e - d}} + \epsilon_{d, \delta})$$

where $\epsilon_{d, \delta}$ is the (order-of) regret bound for the inner-loop (on the subspace $\mathbb{U}_s = \mathfrak{b}_s + \text{span}(\mathfrak{h}_s^0, \mathfrak{h}_s^1, \dots, \mathfrak{h}_s^{d-1})$, not the whole space $L_2(\mathbb{A})$), $(\mathbf{g}_{[s]}^*, \mathbf{y}_{[s]}^*)$ is the best solution found up to the start of iteration s , and $\llbracket \cdot \rrbracket$ is the Iverson bracket.

Proof: The proof may be found in the supplementary material. It is based around the proof of proposition 1 from [Kirschner et al. 2019], with some novel aspects. \square

Note that, unlike LineBO, we do not build-in a requirement that the inner loop terminate with $\text{err}(\mathbf{g}_s^*) < \epsilon$ for some fixed ϵ . Instead, $\epsilon_{d, \delta}$ is used, which is the (order-of) regret bound on the inner loop. If the simple regret test is implemented on the inner loop then $\epsilon_{d, \delta} = \epsilon$. An alternative, fixed budget strategy is also discussed below. Also unlike LineBO the exponent in the regret bound includes the dimension d of the random subspaces. At one extreme, if $d = 1$ and we use the inner-loop convergence condition $\text{err}(\mathbf{g}_s^*) < \epsilon$, then theorem 1 is essentially the same as Proposition 1 in [Kirschner et al. 2019] for LineBO with $\epsilon_{d, \delta} = \epsilon$. In this case the inner loop may be expected to take $T \in \mathcal{O}(\epsilon^{-\frac{2}{1-2\kappa}})$ iterations to complete, and the overall number of function evaluations required by the algorithm is $\mathcal{O}(S \epsilon^{-\frac{2}{1-2\kappa}})$ [Kirschner et al. 2019], where $\kappa \in (0, 0.5)$ is a function of the covariance K . If instead $d = 1$ and the inner loop is allocated a fixed budget of T iterations then we find $\epsilon_{1, \delta} \in \mathcal{O}(T^{\kappa - \frac{1}{2}})$, and the algorithm will make precisely ST function evaluations. At the opposite extreme, if $d = d_e$ then the first term in the regret bound in theorem 1 disappears entirely and the regret is entirely due to $\epsilon_{d_e, \sigma}$. This case is analogous to REMBO, where we know that, with probability 1, any random basis suffices to capture the necessary variation of f . Note that in this case we may set $S = 1$ without affecting our regret bound. The regret bound in this case collapses to precisely the standard regret bounds found in for example [Srinivas et al. 2012].

Between these extremes the algorithm may be expected to act somewhat like a combination of LineBO and REMBO, although of course if d_e is too large - say $d_e \gtrsim 10$ - then setting $d = d_e$ will not be practical, so in this case multiple outer-loop iterations ($S > 1$) will be required.

6 Experimental Results

We consider simulated and real-world experiments. In our simulated experiment we take a draw \mathbf{q} from a GP and then attempt to reconstruct this draw (that is, find \mathbf{g} such that

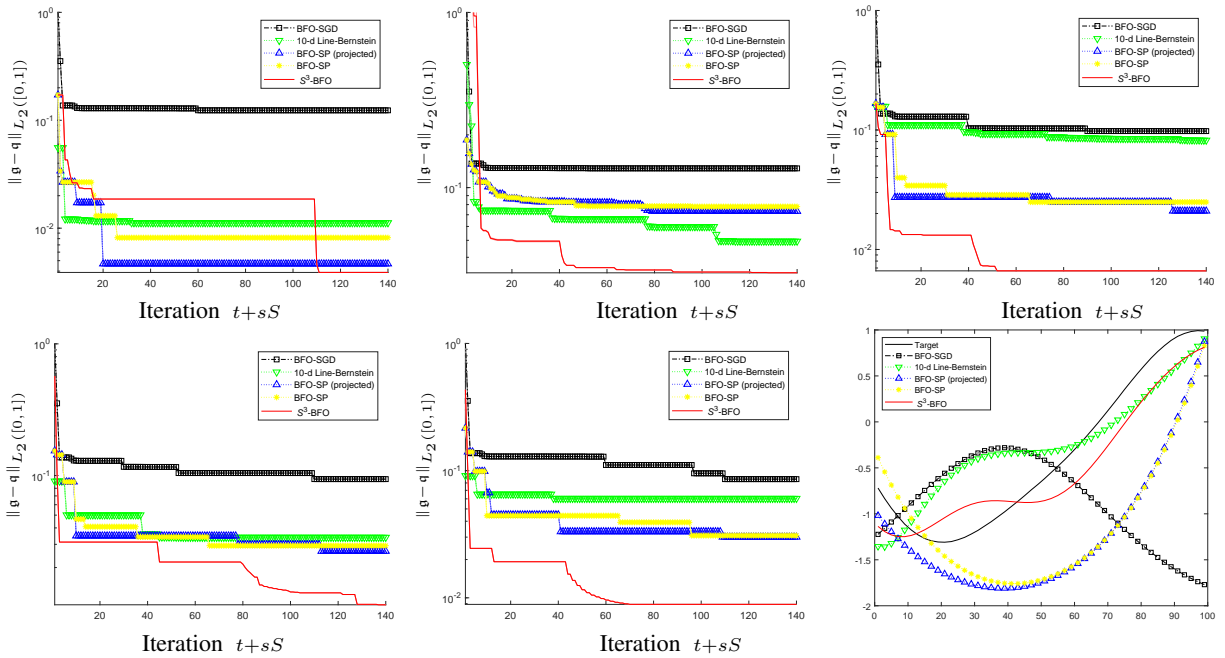


Figure 2: Results for simulated experiments. The top row shows the convergence of $\|\mathbf{g} - \mathbf{q}\|_{L_2([0,1])}$ for three draws with the SE kernel with $\gamma = 1$, $\gamma = 0.3$ and $\gamma = 0.1$ for the different algorithms, while the bottom row shows same for Matern 1/2 and 3/2 (with $\gamma = 0.3$), respectively, and examples of functions found by the various algorithms compared to the target function for a draw from SE GP with $\gamma = 0.3$ (corresponding functions to top row, centre).

$\mathbf{g} = \mathbf{q}$) without explicit knowledge of \mathbf{q} , but with the ability to test/calculate $\|\mathbf{g} - \mathbf{q}\|_{L_2(\mathbb{A})}$. Our two real-world experiments are finding the optimal precipitation strengthening function for a metallic alloy of Aluminium and finding the optimal rate scheduling for deep network training.

All optimisers were implemented in and run with SVMHeavy v7 [Shilton 2001–2020] (code available at <https://github.com/apshsh/SVMHeavy>), excepting the KWN implementation, which is proprietary at present.

We have compared our method with the following: 10-d-Line-Bernstein, which tunes the weights of a 10th order Bernstein polynomial approximation using LineBO; BFO-SP, which implements Vellanki’s algorithm [Vellanki et al. 2019]; BFO-SP projected, which is like BFO-SP but models f in function space as per our algorithm; and BFO-SGD, which is our implementation of [Vien et al. 2018]’s algorithm. All models were based on variants of the SE kernel (real, L_2 or RKHS), and all experiments were repeated 5 times to generate error bars. See supplementary for further details on experimental setup.

6.1 Simulated experiment

The aim of this experiment is to investigate the role of experimenter beliefs in functional optimisation, so for the purposes of this experiment we assume that the experimenter has a good intuitive understanding of the expected lengthscale, smoothness etc (in the form of a covariance function) that cannot be directly used in the alternative methods. To achieve this, we consider function reconstruction - that is, given a target function $\mathbf{q} : [0, 1] \rightarrow \mathbb{R}$, we aim to solve the functional

optimisation problem:

$$\mathbf{g}^* = \operatorname{argmax}_{\mathbf{g}: [0,1] \rightarrow \mathbb{R}} \|\mathbf{g} - \mathbf{q}\|_{L_2([0,1])}$$

As our target functions we have used draws from three Gaussian process, $\mathbf{q} \sim \mathcal{GP}(0, k)$, where $k(x, x') = \exp(\frac{1}{2\gamma}(x - x')^2)$ and $\gamma = 1$, $\gamma = 0.3$ and $\gamma = 0.1$, respectively, as well a draw from a Gaussian process $\mathbf{q} \sim \mathcal{GP}(0, \kappa)$, where κ is Matern-1/2 kernel (with $\gamma = 0.3$), and another where κ is a Matern-3/2 kernel (with $\gamma = 0.3$). In these experiments we assume the experimenter has a good intuition regarding the target function, so the covariance κ is the same as the GP k from which the target was drawn.

Figure 2 shows convergence results for the functions drawn from a GP for different lengthscales, along with a sample of the functions found by the difference approaches (first run in sequence). We note that most methods perform reasonably for the longest lengthscale, which represents the simplest function to approximate. As the lengthscale is shortened we see that our method continues to perform well due to the incorporation of experimenter knowledge, while the alternatives become progressively less accurate. For 10-d-Line-Bernstein this is because the Bernstein polynomial of that order is unable to capture the complexity resulting from the shorter length-scale; and likewise for the BFO-SP variants, although the algorithm is designed to tune the complexity as required, this takes some time, whereas in our algorithm the experimenter intuition is built in. Finally, figure 2, bottom right, shows the best functions found by each algorithm in the first simulation run.

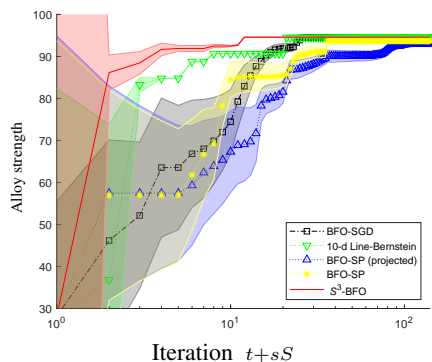


Figure 3: Convergence of precipitation-strengthening. As the alloy strength is highly dependent on the temperature profile there is large variance in strength in the early stages depending on the (random) set of initial observations.

6.2 Precipitation Strengthening in Al-Sc Alloy

Heat treatment of alloys makes them stronger by providing a desired grain structure through precipitation of different crystal structures. Normally, the alloy is heated to a high temperature to first homogenise the structure, then taken through a series of temperature to achieve desired pattern of precipitates. For Al-Sc alloy precipitation strengthening has been proven to be particularly effective [Knipling et al. 2006, 2011, Seidman et al. 2002]; however, as scandium is expensive and the experimental process time-consuming there has been relatively little work in the determination of optimal temperature profile [Deane et al., Vahid et al. 2018, Vellanki et al. 2017].

In this experiment we model the precipitation-strengthening process using Kampmann and Wagner’s numerical model (KWN) [Wagner et al. 2001, Knipling et al. 2010]. This model was implemented in MATLAB and allows us to predict the final strength of the alloy processed according to a given temperature profile (suitably discretized, in our experiments using 100 timepoints). As shown in figure 3, our algorithm converges more quickly than the alternatives. As for the simulated experiment, in this case BFO-LB10 (LineBO to tune the weights of a 10th order Bernstein polynomial) converges second fastest, followed by Vellanki’s method (BFO-SP and BFO-SP (projected)).

6.3 Learning Rate Schedule Optimisation

As noted in [Bengio 2012], and following [Vellanki et al. 2019], stochastic gradient descent (SGD) works better if the learning rate is varied as a function of training duration. In this experiment we optimise the learning rate for a neural network trained on the MNIST dataset (other parameters being kept constant). As a baseline we compare results achieved with our method, and the other baselines already described, with SGD using learning rate 0.1 (decaying exponentially as per [Vellanki et al. 2019]) and momentum 0.8, and Adam with default hyper-parameters [Kinga and Adam 2015]. Unlike [Vellanki et al. 2019] we do not enforce a decreasing rate prior for any of the methods compared.

Results are shown in table 1 (results for SGD, Adam and

SGD	1.26%
Adam	0.86%
BFO-SGD*	0.87%
10-d Line-Bernstein	0.78%
BFO-SP (projected)	0.78%
BFO-SP	0.77%
S^3 -BFO	0.76%

Table 1: Validation error of MNIST neural network for different learning rate schedules (*results from [Vien et al. 2018]).

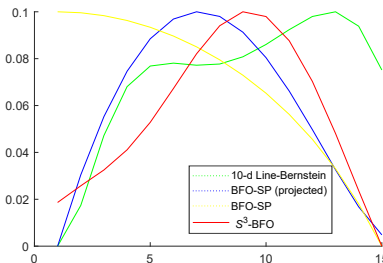


Figure 4: Scheduling functions found by optimisers.

BFO-SGD are sourced from [Vien et al. 2018, Vellanki et al. 2019]). Note that our method achieves the lowest validation error of all approaches considered ([Vellanki et al. 2019] achieves a better result, but only by applying decreasing prior). Actual learning rate schedules are shown in figure 4 (learning rate schedule for BFO-SGD can be found in [Vellanki et al. 2019, Vien et al. 2018]). It is perhaps interesting to note that most solutions found are a simple rise/fall function with a single peak.

7 Conclusion

We have proposed an algorithm for Bayesian functional optimisation - that is, optimisation problems such as finding the best temperature profile for alloy heat treatment, where experiments are expensive/time-consuming and results are noisy. Our algorithm allows the experimenter to express prior beliefs regarding the solution in the form of a covariance function, specifying e.g. length-scale, smoothness, etc. Guided by this prior, our algorithm generates a sequence of finite-dimensional random subspaces, applying standard Bayesian optimisation on each and then building the next subspace from the best solution found. We have presented a sub-linear regret bound for our algorithm and provided experimental results on simulated and real-world experiments, namely simulated function mapping, finding the optimal precipitation-strengthening function for an aluminium alloy, and learning-rate scheduling for deep-network training.

References

- N. Aronszajn. Theory of reproducing kernels. *Transactions of the American Mathematical Society*, 68:337–404, Jan–Jun 1950.
- Yoshua Bengio. Practical recommendations for gradient-based training of deep architectures. In *Neural networks: Tricks of the trade*, pages 437–478. Springer, 2012.
- Eric Brochu, Vlad M. Cora, and Nando de Freitas. A tutorial on bayesian optimization of expensive cost functions, with applications to active user modeling and heirarchical reinforcement learning. eprint arXiv:1012.2599, arXiv.org, December 2010.
- T. M. Cover and J. A. Thomas. *Elements of Information Theory*. Wiley Interscience, New York, 1991.
- Kyle Deane, Vu Nguyen, Santu Rana, Sunil Gupta, Svetha Venkatesh, and Paul G. Sanders. Utilization of bayesian optimization and KWN modeling for increased efficiency of Al-Sc precipitation strengthening. Submitted to Metallurgical and Materials Transactions B.
- Kenneth E. Iverson. *A Programming Language*. Wiley, 1962.
- Carl Jidling, Niklas Wahlström, Adrian Wills, and Thomas B. Schön. Linearly constrained gaussian processes. In *Advances in Neural Information Processing Systems*, pages 1215–1224, 2017.
- Donald R. Jones, Matthias Schonlau, and William J. Welch. Efficient global optimization of expensive black-box functions. *Journal of Global optimization*, 13(4):455–492, 1998.
- D. Kinga and J. B. Adam. A method for stochastic optimization. In *Conference on Learning Representations (ICLR2015)*, 2015.
- Johannes Kirschner, Mojmír Mutný, Nicole Hiller, Rasmus Ischebeck, and Andreas Krause. Adaptive and safe bayesian optimization in high dimensions via one-dimensional subspaces. *arXiv preprint arXiv:1902.03229*, 2019.
- K. E. Knipling, D. C. Dunand, , and Seidman D. N. Criteria for developing castable, creep-resistant aluminium-based allows - a review. *Zeitschrift für Metallkunde (Materials Research and Advanced Techniques)*, 97(3):246–265, Mar 2006.
- K. E. Knipling, R. A. Karnesky, C. P. Lee, D. C. Dunand, and D. N. Seidman. Precipitation evolution in Al-0.1Sc, Al-0.1Zr and Al-0.1Sc-0.1Zr (at.%) alloys during isochronal aging. *Acta Materialia*, 58(15):5184–5195, Sep 2010.
- K.E. Knipling, D.N. Seidman, and D.C. Dunand. Ambient- and high-temperature mechanical properties of isochronally aged Al-0.06Sc, Al-0.06Zr and Al-0.06Sc-0.06Zr(at.%) alloys. *Acta Materialia*, 59(3):943–954, Feb 2011.
- Harold J. Kushner. A new method of locating the maximum point of an arbitrary multipeak curve in the presence of noise. *Journal of Basic Engineering*, 86(1):97–106, 1964.
- David J. C. MacKay. Introduction to gaussian processes. *NATO ASI Series F Computer and Systems Sciences*, 168, 1998.
- Charles A. Micchelli, Yuesheng Xu, and Haizhang Zhang. Universal kernels. *Journal of Machine Learning Research*, 7, 2006.
- Jonas Mockus. Bayesian heuristic approach to global optimization and examples. *Journal of Global Optimization*, 22(1–4):191–203, 2002.
- Carl Edward Rasmussen and Christopher K. I. Williams. *Gaussian Processes for Machine Learning*. MIT Press, 2006.
- Jaakko Riihimäki and Aki Vehtari. Gaussian processes with monotonicity information. In *Proceedings of the thirteenth international conference on artificial intelligence and statistics*, pages 645–652, 2010.
- Matthias W. Seeger, Sham M. Kakade, and Dean P. Foster. Information consistency of nonparametric gaussian process methods. *IEEE Transactions on Information Theory*, 54(5):2376–2382, May 2008.
- D. N. Seidman, E. A. Marquis, and D .C. Dunand. Precipitation strengthening at ambient and elevated temperatures of heat-treatable Al(Sc) alloys. *Acta Materialia*, 50(16):4021–4035, Sep 2002.
- Alistair Shilton. SVMHeavy: SVM, machine learning and optimisation library. <https://github.com/apshsh/SVMHeavy>, 2001–2020.
- Niranjan Srinivas, Andreas Krause, Sham M. Kakade, and Matthias W. Seeger. Information-theoretic regret bounds for gaussian process optimization in the bandit setting. *IEEE Transactions on Information Theory*, 58(5):3250–3265, May 2012.
- Bharath K. Sriperumbudur, Kenji Fukumizu, and Gert R. G. Lanckrie. Universality, characteristic kernels and rkhs embedding of measures. *Journal of Machine Learning Research*, 12, 2011.
- Alireza Vahid, Santu Rana, Sunil Gupta, Pratibha Vellanki, Svetha Venkatesh, and Thomas Dorin. New bayesian-optimization-based design of high-strength 7xxx-series alloys from recycled aluminum. *JOM*, 70(11):2704–2709, Nov 2018.
- Prathiba Vellanki, Santu Rana, Sunil Gupta, David Rubin de Celis Leal, Alessandra Sutti, and Svetha Height, Murray Venkatesh. Bayesian functional optimisation with shape prior. In *Proceedings of the AAAI Conference on Artificial Intelligence*, 2019.
- Pratibha Vellanki, Santu Rana, Sunil Gupta, David Rubin, Alessandra Sutti, Thomas Dorin, Murray Height, Paul Sanders, and Svetha Venkatesh. Process-constrained batch bayesian optimisation. In *Advances in Neural Information Processing Systems*, pages 3414–3423, 2017.
- N. A. Vien, H. Zimmermann, and M. Toussaint. Bayesian functional optimization. In *Proceedings Of The Thirty-Second AAAI Conference on Artificial Intelligence*, pages 4171–4178, November 2018.
- Richard Wagner, Reinhard Kampmann, and Peter W. Voorhees. Homogeneous second-phase precipitation. *Phase transformations in materials*, 5:309, 2001.
- Ziyu Wang, Masrou Zoghi, Frank Hutter, David Matheson, and Nando De Freitas. Bayesian optimization in high dimensions via random embeddings. In *Twenty-Third International Joint Conference on Artificial Intelligence*, 2013.

8 Supplementary: Caching and Optimisation

To improve calculation speed, in our implementation we pre-define a grid $\{\mathbf{c}^i \in \mathbb{A} = [0, 1]^m \subset \mathbb{R}^m | i \in \mathbb{N}_N\}$ on \mathbb{A} as an even grid of $N^{1/m}$ points per axis in $\mathbb{A} \subset \mathbb{R}^m$. Specifically, assuming \mathbb{A} is an m -dimensional unit hypercube, an even grid of $N^{1/m}$ points per axis with spacing $\tau = N^{-1/m}$ (see below). This allows us to approximate points $\mathbf{g} \in L_2(\mathbb{A})$ using $\mathbf{g} \in \mathbb{R}^N$.

The set of initial observations $\mathbb{D}_{[0]}$ are sampled on our grid before entering the algorithm, so \mathbf{g} is represented as $\mathbf{g}_i = \mathbf{g}(\mathbf{c}_i)$, $\forall (\mathbf{g}, y) \in \mathbb{D}_{[0]}$, which also gives us a sampled form $\mathbf{b}_0 = \mathbf{g}_{[0]}^*$ of \mathbf{b}_g for the first (outer) iteration ($s = 0$). To draw basis functions $\mathbf{h}_s^j \sim \mathcal{GP}(0, \kappa)$ in our algorithm we draw an N -dimensional vector:

$$\mathbf{h}_s^j := \begin{bmatrix} \mathbf{h}_s^j(\mathbf{c}^0) \\ \mathbf{h}_s^j(\mathbf{c}^1) \\ \vdots \end{bmatrix} \sim \mathcal{N} \left(\mathbf{0}, \begin{bmatrix} \kappa(\mathbf{c}^0, \mathbf{c}^0) & \kappa(\mathbf{c}^0, \mathbf{c}^1) & \dots \\ \kappa(\mathbf{c}^1, \mathbf{c}^0) & \kappa(\mathbf{c}^1, \mathbf{c}^1) & \dots \\ \vdots & \vdots & \ddots \end{bmatrix} \right)$$

This allows us to evaluate \mathbf{g} on our grid (and cache for later):

$$\mathbf{g} := [\mathbf{g}(\mathbf{c}^0) \ \mathbf{g}(\mathbf{c}^1) \ \dots]^T = \mathbf{b}_s + \sum_j \lambda_j^t \mathbf{h}_s^j$$

and the process may be repeated for subsequent iterations. It follows that we can easily approximate:

$$\|\mathbf{g} - \mathbf{g}'\|_{L^2(\mathbb{A})}^2 \approx \|\mathbf{g} - \mathbf{g}'\|_{2\tau^m}^2 \quad (8)$$

and thus avoid the need to (a) repeatedly re-evaluate our basis functions \mathbf{h}_s^j on our grid and (b) calculate lengthy weighted sums of basis elements when evaluating \mathbf{g} or evaluating the covariance matrix on our grid.

The number of points N required to attain reasonable accuracy in our approximation (8) depend on the characteristics of the (tested) functions $(\mathbf{g}, \cdot) \in \mathbb{D}$. In our algorithm these lie in the span of a set of draws from $\mathcal{GP}(0, \kappa)$, and so inherit their characteristics from the covariance prior κ . Thus if κ is has length-scale γ then it seems reasonable to select $N \approx (D/\gamma)^m$ for some constant D . However this does not *guarantee* the accuracy of (8), as $\mathbf{g} \sim \mathcal{GP}(0, \kappa)$ only implies that \mathbf{g} is likely to have characteristics suitable for such an approximation - for example, for an SE kernel κ , the space of possible draws from $\mathcal{GP}(0, \kappa)$ is *independent* of the length-scale γ (the SE kernel is universal [Micchelli et al. 2006, Sriperumbudur et al. 2011]), so even if the particular prior used in our algorithm has a long length-scale γ it is possible (though unlikely) that our algorithm will explore regions that vary on a much shorter scale than we might naively expect. In practice we recommend being generous when selecting N as the complexity of all relevant operations in our algorithm (weighted sums and (8)) scale linearly with N , so the penalty for “overdoing it” to ensure accurate approximation in (8) is relatively small (for example in our experiments we use $N = 100$).

9 Supplementary: Convergence Analysis - Proof of Theorem 1

We begin by proving some preliminary results. We define $\mathcal{G}_{\kappa, d}(\mathbf{b})$ to be the distribution of random subspaces of $L^2(\mathbb{A})$ of the form $\mathbf{b} + \text{span}(\mathbf{h}^0, \mathbf{h}^1, \dots, \mathbf{h}^{d-1})$, where \mathbf{b} is some

fixed “origin” point and $\mathbf{h}^0, \mathbf{h}^1, \dots, \mathbf{h}^{d-1} \sim \mathcal{GP}(0, \kappa)$. For each outer-loop iteration s of algorithm 2, the inner loop performs Bayesian Optimisation on a subspace $\mathbb{U}_s \sim \mathcal{G}_{\kappa, d}(\mathbf{b}_s)$. For notational convenience we define $\mathbb{U}_{[s]} = \cup_{i \in \mathbb{N}_s} \mathbb{U}_i$, $\mathbf{x}_s^* = \arg \min_{\mathbf{x} \in \mathbb{U}_s} f(\mathbf{x})$, and $\mathbf{x}_{[s]}^* = \arg \min_{\mathbf{x} \in \mathbb{U}_{[s]}} f(\mathbf{x})$. We have the results (it seems probable that lemma 1 is “well known”, but we have been unable to find a reference):

Lemma 1 *Let $\mathbb{U} \subseteq \mathbb{V} = \{\mathbf{v} \in \mathbb{R}^{d_e} | \|\mathbf{v}\|_2 \leq L\}$, where $\mathbb{U} = \text{span}(\mathbf{u}^0, \mathbf{u}^1, \dots, \mathbf{u}^{d-1}) + \mathbf{b} \cap \mathbb{V}$, $\mathbf{u}^i \perp \mathbf{u}^j \ \forall i \neq j \in \mathbb{N}_d$, $\mathbf{u}^i \sim \mathcal{U}_i \ \forall i \in \mathbb{N}_d$, $\mathbf{b} \sim \mathcal{B}$, for smooth distributions $\mathcal{U}_i, \mathcal{B}$. Then the probability that \mathbb{U} intersects the d_e -ball of radius $r = \beta L$, $\beta \in (0, 1]$, at the origin is at least $\Omega(\beta^{d_e-d})$ if $d < d_e$, 1 otherwise.*

Proof: Denote the probability of intersection by $\zeta_{d, d_e}(\beta)$. With probability 1 we have that $\|\mathbf{u}^i\|_2 \neq 0 \ \forall i \in \mathbb{N}_d$. Hence we may assume $\dim(\mathbb{U}) = d$.

If $d = d_e$ then $\mathbb{U} = \mathbb{V}$ and $\zeta_{d_e, d_e}(\beta) = 1$ trivially. If $d = 0$ then the probability of intersection is precisely the probability that a point selected from a smooth distribution falls into an d_e -ball of radius $r = \beta L$, which goes as the ratio of the measure of the d_e -ball and the measure of \mathbb{V} - that is, $\zeta_{0, d_e}(\beta) = \Omega(\beta^{d_e})$.

Otherwise if $0 < d < d_e$ note that, as both \mathbb{V} and the d_e -ball are rotationally symmetric about the origin, we may always assume that $\mathbf{u}^i = [\delta_{0,i} \ \delta_{1,i} \ \dots \ \delta_{d-1,i} \ \mathbf{0}] \tilde{u}_i$, $i \in \mathbb{N}_d$, where $\delta_{i,j}$ is the Kronecker-delta symbol. Hence, writing $\mathbf{b} = [\hat{\mathbf{b}} \ \check{\mathbf{b}}]$, $\hat{\mathbf{b}} \in \mathbb{R}^d$, $\check{\mathbf{b}} \in \mathbb{R}^{d_e-d}$, and noting that $\tilde{u}_i \neq 0 \ \forall i \in \mathbb{N}_d$ with probability 1 and $\check{\mathbf{b}} \sim \check{\mathcal{B}}$ (conditioned on $\hat{\mathbf{b}}$), we have with probability 1:

$$\begin{aligned} \zeta_{d, d_e}(\beta) &= \Pr \left(\min_{\gamma \in \mathbb{R}^d} \left\| \begin{bmatrix} \hat{\mathbf{b}} + \gamma \odot \tilde{\mathbf{u}} \\ \check{\mathbf{b}} \end{bmatrix} \right\|_2 \leq \beta L \right) \\ &= \Pr (\|\check{\mathbf{b}}\|_2 \leq \beta L) \end{aligned}$$

where \odot is the elementwise product and the minima is attained with $\gamma_i = -\hat{b}_i / \tilde{u}_i \ \forall i \in \mathbb{N}_d$. However this is precisely equivalent to the $d = 0$ case with decreased d_e , hence $\zeta_{d, d_e}(\beta) = \zeta_{0, d_e-d}(\beta) = \Omega(\beta^{d_e-d})$ when $0 < d < d_e$. ■

Lemma 2 (analog of [Kirschner et al. 2019], Lemma 2)

For outer-loop iteration s of algorithm 2:

$$\Pr \left(f(\mathbf{g}^*) - f(\mathbf{g}_{[s]}^*) \leq \tau \right) \geq 1 - \exp(-s\xi(\tau))$$

where $\xi(\tau)$ is a lower bound on:

$$\xi(\tau) \leq \Pr (\exists \mathbf{g} \in \mathbb{U}, f(\mathbf{g}^*) - f(\mathbf{g}) \leq \tau | \mathbb{U} \sim \mathcal{G}_{\kappa, d}(\mathbf{b}))$$

Furthermore if the first-order minimum condition is met at \mathbf{g}^* then $\xi(\tau) = \Omega(\tau^{\frac{d_e-d}{2}})$ if $d < d_e$, $\xi(\tau) = 1$ otherwise.

Proof: The proof follows the approach of [Kirschner et al. 2019], extended to the functional domain. Using the inequality $1 - x \leq e^{-x}$, we have that:

$$\begin{aligned} \Pr(f(\mathbf{g}^*) - f(\mathbf{g}_{[s]}^*) \leq \tau) &= 1 - \Pr(f(\mathbf{g}^*) - f(\mathbf{g}_{[s]}^*) \geq \tau) \\ &= 1 - \prod_{i \in \mathbb{N}_s} \Pr(f(\mathbf{g}^*) - f(\mathbf{g}_i^*) \geq \tau) \\ &\geq 1 - (1 - \xi(\tau))^s \\ &\geq 1 - \exp(-s\xi(\tau)) \end{aligned}$$

Recall that, by definition, $\exists \bar{\mathbf{h}}^0, \bar{\mathbf{h}}^1, \dots, \bar{\mathbf{h}}^{d_e-1} \in L^2(\mathbb{A})$ such that $\|f(\mathbf{g}_\top + \mathbf{g}_\perp) - f(\mathbf{g}_\top)\|_{L^2(\mathbb{A})} = 0 \forall \mathbf{g}_\top \in \mathbb{T}, \forall \mathbf{g}_\perp \in \mathbb{T}^\perp$, where $\mathbb{T} = \text{span}(\bar{\mathbf{h}}^0, \bar{\mathbf{h}}^1, \dots, \bar{\mathbf{h}}^{d_e-1})$. We adopt the notational convention that $\forall \mathbf{g} \in L^2(\mathbb{A})$, $\mathbf{g} = \mathbf{g}_\top + \mathbf{g}_\perp$ where $\mathbf{g}_\top \in \mathbb{T}, \mathbf{g}_\perp \in \mathbb{T}^\perp$. Define:

$$\mathbb{V}_\tau = \{ \mathbf{g} \in L^2(\mathbb{A}) \mid f(\mathbf{g}^*) - f(\mathbf{g}) \leq \tau \}$$

to be the set of solutions within $\tau \geq 0$ of the optima. As $f(\mathbf{g}) = f(\mathbf{g}_\top)$ it follows that $\mathbb{V}_\tau = \mathbb{V}_{\tau\top} \oplus \mathbb{T}^\perp$, where:

$$\mathbb{V}_{\tau\top} = \{ \mathbf{g}_\top \in \mathbb{T} \mid f(\mathbf{g}^*) - f(\mathbf{g}_\top) \leq \tau \}$$

has dimension d_e . Hence to place a lower bound on $\xi(\tau)$ it suffices to bound the probability that a random d -dimensional linear subspace $\mathbb{U} \sim \mathcal{G}_{\kappa,d}(\mathbf{b})$ projected onto \mathbb{T} (ie. $\mathbb{U}_\top = \{ \mathbf{g}_\top \mid \mathbf{g} \in \mathbb{U} \}$, $\mathbb{U} \sim \mathcal{G}_{\kappa,d}(\mathbf{b})$) intersects $\mathbb{V}_{\tau\top}$. To bound this, define:

$$\tilde{\mathbb{V}}_{\tau,\alpha\top} = \left\{ \mathbf{g}_\top \in \mathbb{T} \mid \frac{\alpha}{2L_{\max}^2} \|\mathbf{g}^* - \mathbf{g}_\top\|_{L^2(\mathbb{A})}^2 \leq \tau \right\}$$

where $\alpha > 0$. Using the fact that f is twice Frechet differentiable we have that $f(\mathbf{g}^* + \mathbf{q}) \geq f(\mathbf{g}^*) - \frac{\alpha}{2L_{\max}^2} \|\mathbf{q}\|_{L^2(\mathbb{A})}^2$ for sufficiently small $\frac{\alpha}{2L_{\max}^2} \|\mathbf{q}\|_{L^2(\mathbb{A})}^2$. Letting $\mathbf{q} = \mathbf{g}_\top - \mathbf{g}^*$ we see that $f(\mathbf{g}^*) - f(\mathbf{g}_\top) \leq \frac{\alpha}{2L_{\max}^2} \|\mathbf{g}_\top - \mathbf{g}^*\|_{L^2(\mathbb{A})}^2$, so $\tilde{\mathbb{V}}_{\tau,\alpha\top} \subseteq \mathbb{V}_{\tau\top}$.

Hence to place a lower bound on $\xi(\tau)$ it suffices to bound the probability that a random d -dimensional linear subspace \mathbb{U}_\top in a d_e -dimensional space intersects a d_e -ball at the origin of radius $\sqrt{2\tau/\alpha}L_{\max}$, which by Lemma 1 is $\Omega(\tau^{\frac{d_e-d}{2}})$ if $d < d_e$ and 1 otherwise, completing the proof. ■

Having established the above result the proof of theorem 1 follows almost precisely that of [Kirschner et al. 2019], proof of proposition 1, excepting that $d_e - 1$ is replaced by $d_e - d$ wherever present, and rather than enforcing an upper bound on ϵ we allow it to vary with order $\epsilon_{d,\delta}$.

10 Supplementary: Details of Experimental Procedure

In the paper we have compared the following methods:

1. S^3 -BFO: our method as described, using a $d = 1$ dimensional search subspace, 5 initial observations, $S = 4$ outer loop iterations, $T = 30$ inner loop iterations (fixed budget on the inner loop), $L^2(\mathbb{R})$ -SE covariance prior K on f with length-scale selected for maximum likelihood at each model update, SE covariance prior κ on \mathbf{g}^* with length-scale 0.3 unless otherwise stated, GP-UCB acquisition function.
2. 10-d-Line-Bernstein: LineBO algorithm used to tune the weights of 10^{th} -order Bernstein polynomial, using 4 lines in sequence, 30 iterations per line (standard GP-UCB BO on each line), where f is modelled on weights of Bernstein polynomial using SE covariance K with length-scale selected for maximum likelihood at each iteration.
3. BFO-SP: Vellanki's algorithm [Vellanki et al. 2019], with f modelled on weights of Bernstein polynomial using SE covariance K with length-scale selected for maximum likelihood at each iterations.

4. BFO-SP (projected): like BFO-SP, except that in this case f has been modelled in function space using $L^2(\mathbb{R})$ -SE covariance prior with length-scale selected for maximum likelihood at each iteration.
5. BFO-SGD: based on [Vien et al. 2018], f modelled in function space using $\mathcal{H}_\kappa(\mathbb{R})$ -SE covariance prior (as per [Vien et al. 2018]) with length-scale selected for maximum likelihood at each iteration, κ is SE covariance with length-scale 0.3 unless otherwise stated. Note that, while we were unable to obtain source code from the authors, every effort has been made to ensure that our implementation matches the description as closely as possible.

When calculating norms in L^2 we have used a uniform grid with spacing $\tau = 0.01$ (so $N = 100$ for a 1-dimensional function) - see section 8 for more information on how this effects our simulation. All experiments were repeated 5 times to obtain error bars. All optimisers and simulators were implemented in and run with SVMHeavy v7 [Shilton 2001–2020] and a proprietary KWN implementation. SVMHeavy is available on github at <https://github.com/apshsh/SVMHeavy>.